April 1999 • NREL/CP-500-26244

Conference Paper

Non-Linear and Linear Model Based Controller Design for Variable-Speed Wind Turbines

M.M. Hand
National Renewable Energy Laboratory

M.J. Balas
Department of Aerospace Engineering Sciences,
University of Colorado

Presented at the 3rd ASME/JSME Joint Fluids Engineering Conference
San Francisco, California
July 18-23, 1999

National Renewable Energy Laboratory
1617 Cole Boulevard
Golden, Colorado 80401-3393

NREL is a U.S. Department of Energy Laboratory
Operated by Midwest Research Institute • Battelle • Bechtel

Contract No. DE-AC36-98-GO10337

NOTICE

Available to DOE and DOE contractors from:
Office of Scientific and Technical Information (OSTI)
P.O. Box 62
Oak Ridge, TN 37831
Prices available by calling 423-576-8401

Available to the public from:
National Technical Information Service (NTIS)
U.S. Department of Commerce
5285 Port Royal Road
Springfield, VA 22161
703-605-6000 or 800-553-6847
or
DOE Information Bridge
http://www.doe.gov/bridge/home.html


Printed on paper containing at least 50% wastepaper, including 20% postconsumer waste

Proceedings of FEDSM99:
3rd ASME/JSME Joint Fluids Engineering Conference
July 18–23, 1999, San Francisco, California

FEDSM99-S295-11

NON-LINEAR AND LINEAR MODEL BASED CONTROLLER DESIGN FOR VARIABLE-SPEED WIND TURBINES

M. Maureen Hand
National Renewable Energy Laboratory
1617 Cole Blvd., Golden, CO 80401
Email: maureen_hand@nrel.gov

Mark J. Balas
Department of Aerospace Engineering Sciences
University of Colorado, Boulder, CO 80309
Email: mark.balas@colorado.edu

ABSTRACT

Variable-speed, horizontal axis wind turbines use blade-pitch control to meet specified objectives for three regions of operation. This paper focuses on controller design for the constant power production regime. A simple, rigid, non-linear turbine model was used to systematically perform trade-off studies between two performance metrics. Minimization of both the deviation of the rotor speed from the desired speed and the motion of the actuator is obtained through systematic selection of proportional-integral-derivative controller gain values. The gain design is performed using a non-linear turbine model and two linear models. The linear models differ only in selection of linearization point. The gain combinations resulting from design based upon each of the three models are similar. Performance under each of the three gain combinations is acceptable according to the metrics selected. The importance of operating point selection for linear models is illustrated. Because the simulation runs efficiently, the non-linear model provides the best gain design, but careful selection of the linearization point can produce acceptable gain designs from linear models.

INTRODUCTION

Utility-scale wind turbine manufacturers have recently begun to explore the advantages of variable-speed operation. Because variable-speed wind turbines have the potential for increased energy capture, controller design has become an area of increasing interest. Blade-pitch regulation provides means for initiating rotation, varying rotational speed to extract power at low wind speeds, and maintaining power production at a maximum level. Controllers must be designed to operate in each of these regions, but this study pertains only to the power regulation regime.

The power regulation regime is entered when the turbine reaches the design rotor speed for maximum power production. Under these conditions, rotational speed is constrained to a specified maximum value through blade-pitch regulation. Fluctuations in wind speed are accommodated to prevent large excursions from the desired rotational speed. Thus the power production is also constrained to a relatively constant level. In addition to maintaining a constant rotational speed, actuator movement must be restrained to prevent fatigue and thermal overload. The combination of maintaining a constant rotational speed and minimizing actuator motion are the control objectives specified for the power regulation regime.

Controller design has centered mainly on simple, linear, proportional-integral-derivative (PID) controllers that are easily implemented in the field environment. Gain selection for these controllers has traditionally been a trial and error process relying on the experience and intuition of the engineers. The systematic method used in this study, reduces the reliance on intuition and results in a controller design that is optimized for the specified performance metrics. This PID controller establishes the baseline performance to which more sophisticated controllers can be compared.

Sophisticated controllers such as state estimation based controllers provide the potential for control of multiple inputs and outputs. These controllers could be used to mitigate fatigue of blades in addition to regulating rotor speed. However, these sophisticated controllers often require a linear model for their design.

A comparison of the PID controller design based upon a non-linear model and the design based upon two linear models is presented in order to illustrate the design's dependence on the model used. Also, a comparison of operating point selection for the linear model is included.

DYNAMIC MODEL

The simple, rigid, non-linear turbine model developed for the purpose of controller design by Kendall et al. (1997), was used for this design study. The geometry and aerodynamic characteristics of the simulated turbine resemble those of a Grumman Windstream-33, 10-m diameter, 20-kW turbine. The National Renewable Energy Laboratory's National Wind

Technology Center modified this turbine to operate at variable speeds using blade-pitch regulation. The original drive-train consisting of a low-speed shaft, gearbox, high-speed shaft, and generator, was replaced with a single, stiff, shaft and direct-drive generator. Because the drive-train compliance was reduced to that of the stiff shaft only, it has been neglected in this model.

The fundamental dynamics of this variable-speed wind turbine are captured with the following simple mathematical model:

$$J_T \dot{\omega}_T = Q_A - Q_E \quad (1)$$

The moment of inertia of the turbine rotor, 1270 kg·m^2, is represented by J_T; ω_T is the angular shaft speed; Q_E is the mechanical torque necessary to turn the generator and was assumed to be a constant value commanded by the generator. Because the generator moment of inertia of a direct-drive turbine is generally several orders of magnitude less than J_T, it has been neglected. The aerodynamic torque, Q_A, is represented by:

$$Q_A = \frac{1}{2}\rho A R c_q(\lambda, \beta) w^2 \quad (2)$$

The air density, ρ, swept area of the rotor, A, and rotor radius, R, are constant. The radius of this particular turbine is 5 m. The wind speed is given by w.

The torque coefficient, c_q, is a highly non-linear function of tip-speed ratio, λ, and blade-pitch angle, β, as illustrated in Figure 1. The tip-speed ratio is defined as the ratio of the blade tip speed to the prevailing wind speed. The surface shows only positive values of c_q because the turbine operates most often in this region. These non-linear aerodynamic characteristics are implemented as a look-up table which was generated using PROPPC (Tangler 1987). This aerodynamics code uses blade-element momentum theory and empirical models that predict stalled operation and blade tip losses.

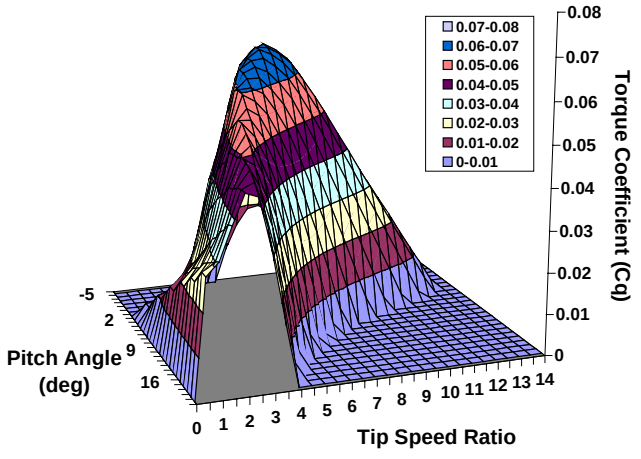

Figure 1. Torque coefficient surface as a function of tip-speed ratio and blade-pitch angle. All negative c_q values have been set to zero.

Linearizing the non-linear turbine dynamics expressed in Equation 1 results in the following assuming that $Q_A|_{OP}=Q_E|_{OP}$;

$$J_T \Delta \dot{\omega}_T = \gamma \Delta \omega_T + \alpha \Delta w + \delta \Delta \beta \quad (3)$$

where the linearization coefficients are given by:

$$\gamma = J_T \left.\frac{\partial \dot{\omega}_T}{\partial \omega_T}\right|_{OP} = \frac{1}{2}\rho A R^2 w_{OP} \left.\frac{\partial c_q}{\partial \lambda}\right|_{OP}$$

$$\alpha = J_T \left.\frac{\partial \dot{\omega}_T}{\partial w}\right|_{OP} = \frac{1}{2}\rho A R w_{OP}\left[2c_q\big|_{OP} - \lambda_{OP}\left.\frac{\partial c_q}{\partial \lambda}\right|_{OP}\right]$$

$$\delta = J_T \left.\frac{\partial \dot{\omega}_T}{\partial \beta}\right|_{OP} = \frac{1}{2}\rho A R\, w_{OP}^2 \left.\frac{\partial c_q}{\partial \beta}\right|_{OP}$$

Here, $\Delta\omega_T$, Δw, and $\Delta\beta$ represent deviations from the chosen operating point, ω_{TOP}, w_{OP}, and β_{OP}.

Selection of the operating point is critical to preserving aerodynamic stability in this system. The rotational speed operating point, $\omega_{T\ OP,}$ was selected to be the desired constant speed of the turbine, 105 RPM (11 rad/s). The blade-pitch and wind speed operating points were selected using the power coefficient surface shown in Figure 2. The maximum c_p value over the entire surface occurs at a pitch angle of 3° and a tip-speed ratio of 7. Using the constant rotational speed of 11 rad/s, this tip-speed ratio corresponds to a wind speed of 7.5 m/s. At this point, the turbine would produce maximum power. However, slight deviation from this point toward negative pitch angles could result in stalled blades which dramatically decreases the power produced. It is important to note that stalled blades can also occur in low tip-speed-ratio conditions. In these regions, the torque coefficient surface in Figure 1 has positive slope.

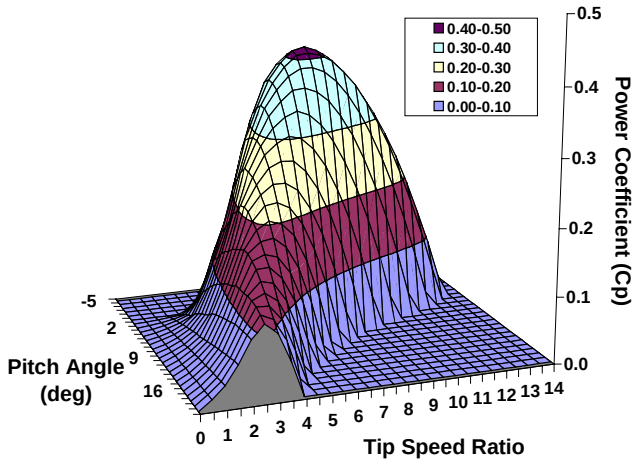

Figure 2. Power coefficient surface as a function of tip-speed ratio and blade-pitch angle. All negative c_p values have been set to zero.

An operating point for linearization must be chosen in a region where deviation in all directions can be tolerated. By increasing the blade-pitch angle from 3° to 9° and maintaining the tip-speed-ratio of 7, the first operating point was selected as shown in Figure 3. At this point on the c_p surface, the power coefficient may be approximated by a relatively flat plane tangent to the surface which is ideal for linearized models. Thus, the operating point labeled Linear I was chosen to be: $\omega_{T\ OP}$ = 11 rad/s; w_{OP} = 7.5 m/s; and β_{OP} = 9°.

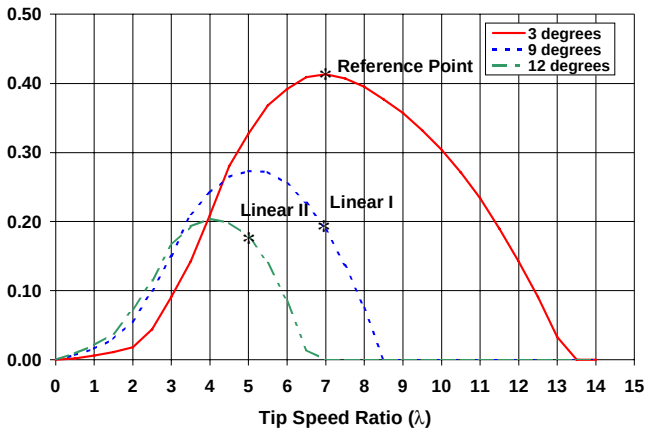

Figure 3. Example of c_P versus λ for three pitch angles.

For comparison, a second operating point was selected. Simply increasing the pitch angle from 9° to 12° and maintaining the tip-speed-ratio of 7 places the point in the negative power coefficient region. By shifting the linearization point in both pitch angle and tip-speed-ratio, the tangent area around the point is maintained near the top of the curve as shown in Figure 3. This tip-speed-ratio of 5 corresponds to a wind speed of 10 m/s when maintaining the rotor speed at 11 rad/s. The second linearization point, Linear II, was selected to be as follows: $\omega_{T\ OP}$ = 11 rad/s; w_{OP} = 10 m/s; and β_{OP} = 12°. The peak of the c_p surface represents the reference values used in the simulation: $\omega_{T\ ref}$ = 11 rad/s; w_{ref} = 7.5 m/s; and β_{ref} = 3°.

The block diagram in Figure 4 illustrates the simulation logic as implemented with MATLAB® Simulink® software. Actual wind data sampled at 1 Hz is the input to the non-linear plant model (either linear model can be substituted for the non-linear aerodynamics block). The turbine speed is fed back, and the reference speed, $\omega_{T\ ref}$, is subtracted from it resulting in $\Delta\omega_T$ (noise in the sensor measurements has been neglected). This rotor-speed error is input to the controller which commands a change in blade-pitch angle, $\Delta\beta$, based on $\Delta\omega_T$. The new pitch angle requested is then $\beta = \Delta\beta + \beta_{ref}$, which is physically limited to angles between 3° and 60°. The actuator operates on a pitch rate command. The pitch rate is determined from the difference between the commanded pitch angle and the measured blade-pitch angle (noise in the measurements is again neglected). The simulation uses a variable step size with a maximum step of 0.05 seconds. A new wind speed is read from the input file when the simulation time step corresponds to the time step of the wind data. A new rotational speed is then determined at the resulting tip-speed ratio and blade-pitch angle.

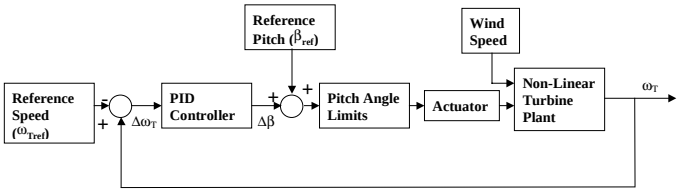

Figure 4. Simulation block diagram.

CONTROLLER DESIGN COMPARISON

In order to compare performance under various gain designs, two metrics were selected. The primary objective of the controller was to maintain a constant rotor speed which was ascertained using the root mean square (RMS) of the rotor speed deviation from the desired constant value of 105 RPM. Additionally, the hydraulic actuator that pitches the blade must be considered. Excessive motion causes the hydraulic fluid to overheat and decreases the fatigue life of the linkage. In order to measure actuator motion, the Actuator Duty Cycle (ADC) was proposed by Kendall et al. (1997). This measure is simply the total number of degrees pitched over the time period of the simulation. Both the RMS speed error and the actuator duty cycle must be minimized to produce acceptable operating conditions.

Using the systematic design methodology developed by Hand , (1998), PID controller gains were selected for each of the three models. This methodology exploits the simplicity of the models and the resulting short run times. Surfaces illustrating the RMS speed error and actuator duty cycle values for various combinations of proportional (k_P) and derivative (k_D) gains at a specified integral gain (k_I) were created. This was done for k_I values from 1 to 20. These surfaces were generated using the non-linear turbine plant model as well as both of the linear turbine models. Five different wind input files were used, and the average response under all gain combinations was calculated for both metrics. By varying all three gains over a wide range of values and calculating both metrics, trade-off studies are performed to determine optimal operating conditions.

Figure 5 illustrates the turbine performance as simulated using the non-linear turbine plant for a variety of proportional and derivative gain combinations at an integral gain of 5. Similar surfaces generated at k_I = 1 and k_I = 10 were created for comparison. For the surfaces shown in Figure 5, the ADC is minimized in the "bucket" that appears in the region of moderate gain values of 5-10 for both k_P and k_D. The RMS speed error surface exhibits a sharply increasing slope for k_P < 7. Then it levels off around k_P = 7 and slopes gently toward 0

as the k_P gain increases. When the integral gain is 1, the RMS speed error surface does not level off until $k_P > 20$, but the ADC corresponding to the region of the "bucket" at $k_I = 5$ is similar to that at $k_I = 1$. As the integral gain increases to 10, the "bucket" evident in the ADC surface forms at gradually higher ADC values. In an attempt to minimize both metrics simultaneously, the integral gain was established at 5 deg/rad.

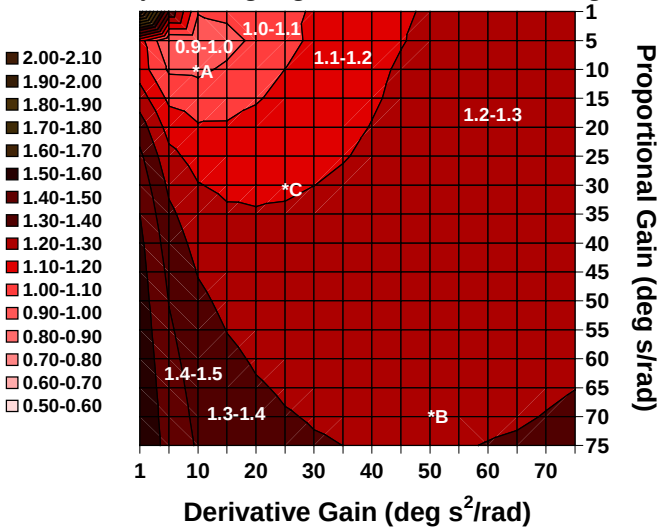

(a) Actuator duty cycle (deg/s)

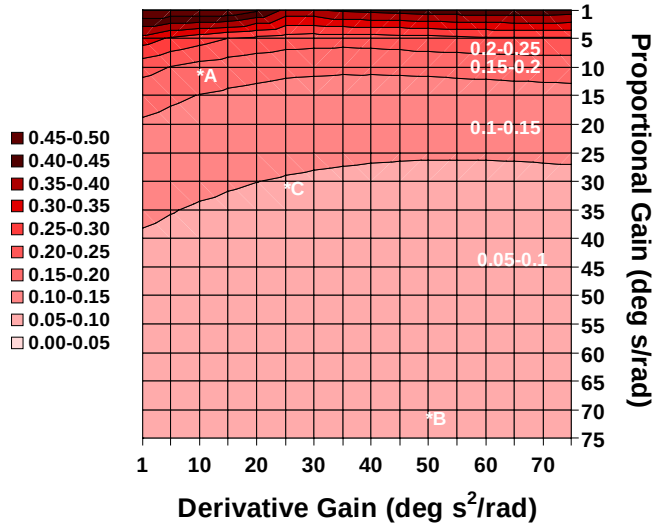

(b) RMS rotor speed error (rad/s)

Figure 5. Performance metric surfaces generated using the non-linear turbine model for k_I=1 deg/rad.

In order to determine the dominant metric, points were selected on the surface, and time-series traces were created. Point A was selected to minimize the ADC; Point B was selected to minimize the RMS speed error; Point C was a compromise in the lowest RMS error contour and the corresponding ADC contour.

Time-series traces resulting from simulating turbine operation under the most extreme wind input case are shown in Figure 6 for each of the three gain combinations, A, B, and C. The rotor speed shown in Figure 6 (b) varies too much for gain combination A (when Actuator Duty Cycle is minimized). The pitch rate, Figure 6 (d), provides a visualization of actuator motion over the duration of the simulation. The excess motion at 50 seconds under the gain combination B (when RMS speed error is minimized) leads to unacceptably high Actuator Duty Cycle values. Thus, gain combination C, the compromise between the two metrics produces acceptable speed regulation as well as minimal actuator motion.

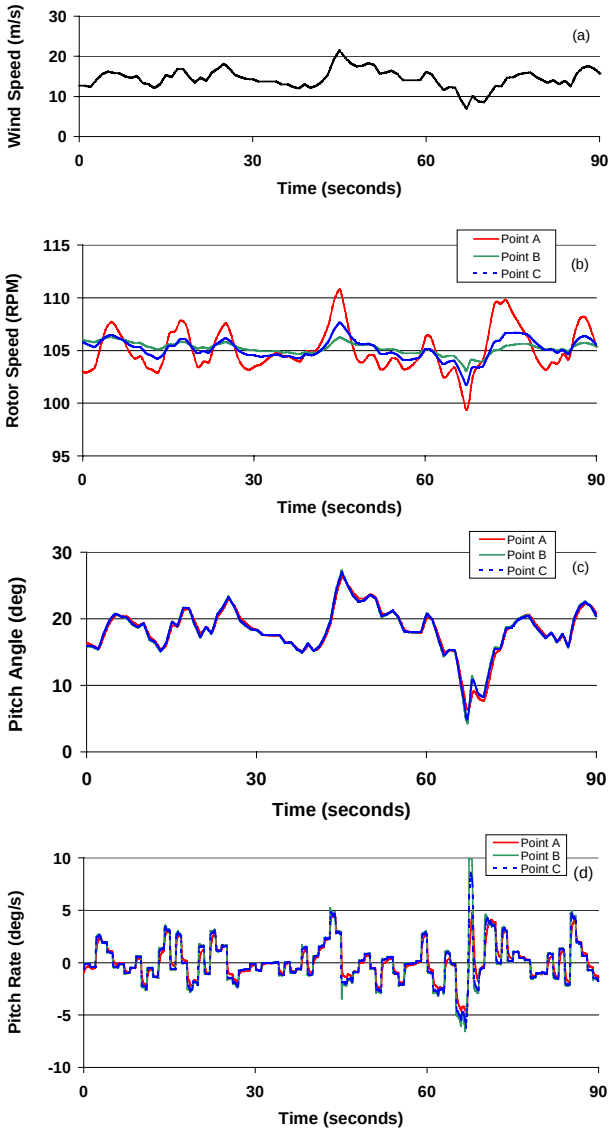

Figure 6. Time-series traces of turbine performance.

Similar surfaces were generated using both of the linear turbine models. The results from five wind input cases were averaged to produce each point on the surface. Again, the k_I=5

surface provided the best simultaneous minimization of both metrics. Points A, B, and C were selected in the same manner as for the surfaces generated by the non-linear turbine model. The surfaces for the Linear I model and the Linear II model are shown in Figures 7 and 8 respectively.

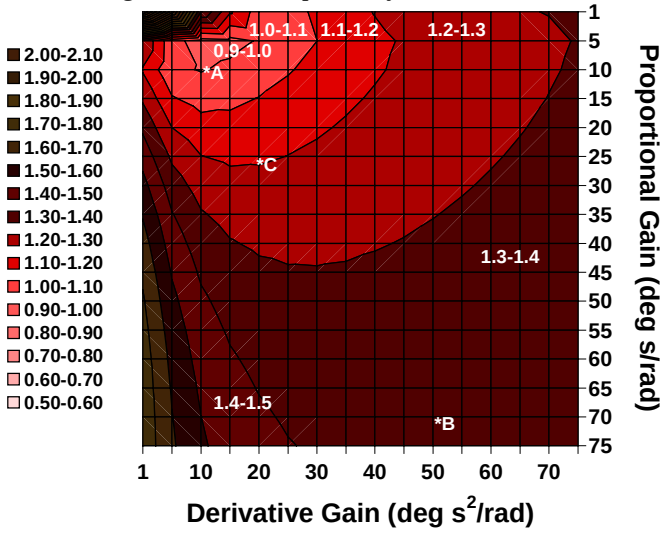

(a) Actuator duty cycle (deg/s)

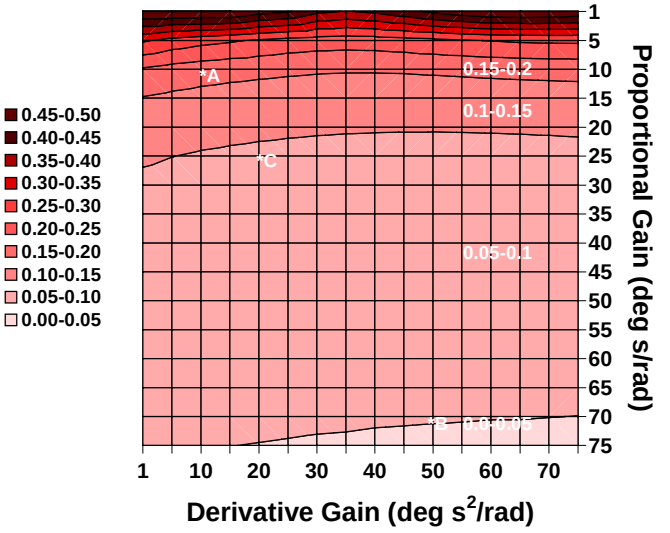

(b) RMS speed error (rad/s)

Figure 7. Performance metric surfaces generated using the first linear model ($\omega_{T\,OP}$ = 11 rad/s; w_{OP} = 7.5 m/s; and β_{OP} = 9°) for k_I=5 deg/rad.

In general, the surfaces created by all three models are similar. The second linear model surfaces more closely represent those generated by the non-linear model. The actuator duty cycle increases toward the perimeters of the surface most rapidly when the first linear model is used, and the corresponding non-linear model based surface is the flattest. Comparison of the RMS speed error surfaces indicates that the non-linear model generated surface is the flattest, and the second linear model surfaces are the steepest. Thus, in the area surrounding Point C, the models all behave similarly. The greatest differences appear toward the edges of the surfaces.

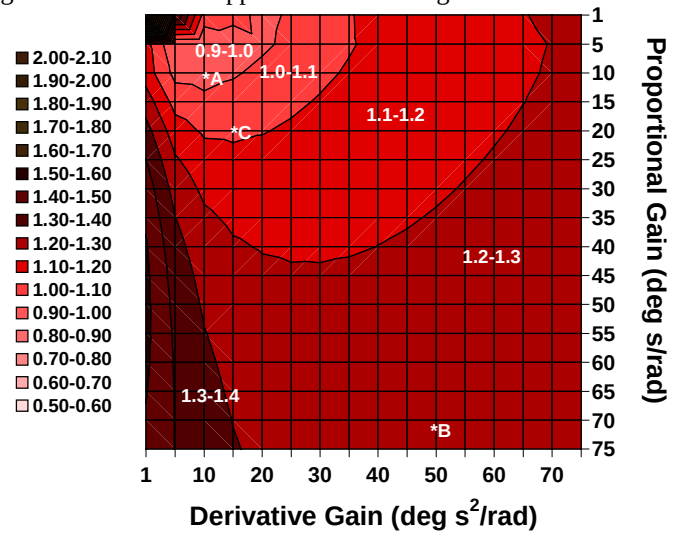

(a) Actuator duty cycle (deg/s)

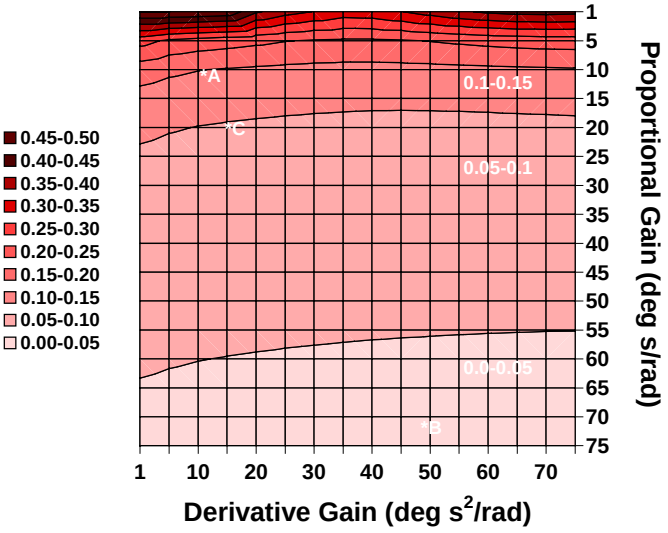

(b) RMS speed error (rad/s)

Figure 8. Performance metric surfaces generated using the second linear model ($\omega_{T\,OP}$ = 11 rad/s; w_{OP} = 10 m/s; and β_{OP} = 12°) for k_I=5 deg/rad.

Comparison of the regions of optimal operation selected using the non-linear model, and the two linear models is shown in Figure 9. The optimal region selected using the second linear model deviates the most from that obtained using the non-linear model. Assuming that the non-linear model provides the best representation of actual turbine operation, time-series traces were created using the optimal gain combination obtained from both linear models. Figure 10 illustrates the time-series turbine behavior when subjected to the most extreme wind speed case. Included in Figure 10 are the time traces produced by the non-

linear plant simulation when the gains are chosen using the non-linear model design approach.

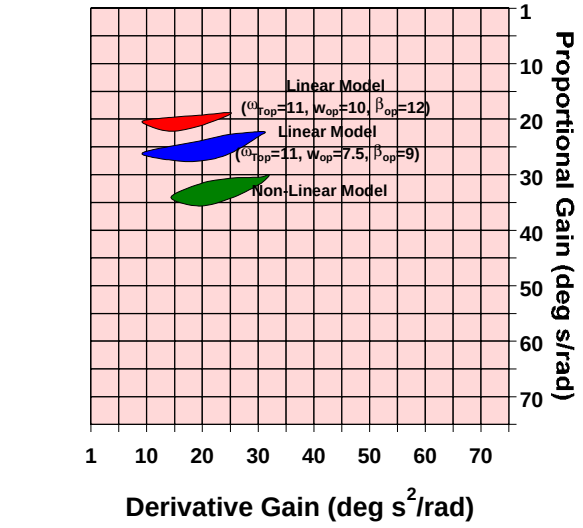

Figure 9. Regions of optimal operation.

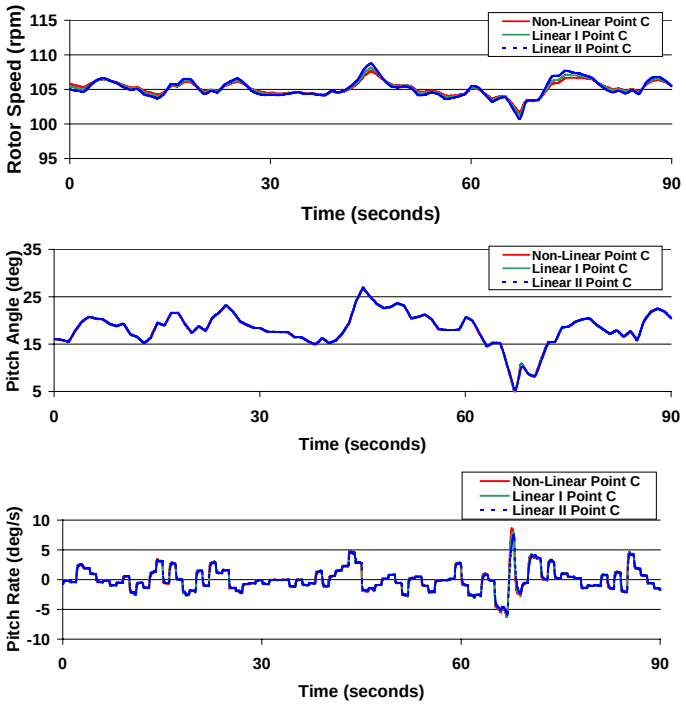

Figure 10. Time-series traces of turbine performance under the optimal gains as determined using each of the three models.

Using the gains selected based on the first linear model, the rotor speed nearly duplicates that of the non-linear model optimal gain combination. The pitch rate traces are very similar for all three gain combinations, but the second linear model-based optimal gains slightly out-perform those from the first linear model design. Again, the blade pitch angles commanded by the controller are nearly identical.

CONCLUSIONS

This systematic approach to PID-controller design provides a means of visually observing the effect of gain changes on both RMS speed error and actuator duty cycle. While these metrics are in opposition by nature, the surfaces permit selection of gain values that produce favorable results for both of the metrics.

The non-linear turbine dynamics simulated with this simple turbine model are easily linearized, but several considerations must be made in order to design a PID controller using a linear model. The optimal region based on the balanced performance of the two metrics shifts with the linearization point selection. The surfaces generated by the linear models tend to slope less gradually toward the perimeters. These differing slopes yield different areas on the surface that provide the desired combination of the two performance metrics. Operating point selection for a linear model is critical in obtaining the best possible performance from this highly non-linear system.

Although the surfaces are relatively flat, performance does vary when gain combinations from different areas of the surface are compared. These small variations may be exacerbated by more complicated turbine dynamics and sensor noise when these gains are implemented in the field. Thus it is assumed that the non-linear model-based design will be superior to the designs that relied upon the linear model.

ACKNOWLEDGMENTS

This work was supported by the U.S. Department of Energy under contract number DE-AC36-98-G010337.

REFERENCES

Hand, M. 1998. "Variable-Speed Wind Turbine Controller Systematic Design Methodology: A Comparison of Non-Linear and Linear Model-Based Designs," Master's Degree Thesis, University of Colorado, Boulder, Colorado, U.S.A.

Kendall, L., Balas, M.J., Lee, Y.J., and Fingersh, L.J. 1997. "Application of Proportional-Integral and Disturbance Accommodating Control to Variable-speed Variable Pitch Horizontal Axis Wind Turbines," Wind Engineering (12:1); pp. 21-38.

Tangler, J.L. 1987. "User's Guide. A Horizontal Axis Wind Turbine Performance Prediction Code for Personal Computers," Solar Energy Research Institute (now known as National Renewable Energy Laboratory), Golden, Colorado, U.S.A.